Determination of Rock Joint Roughness Using Self-affine Fractal Approach

S.M. Hsiung, A. Ghosh, and A.H. Chowdhury
Center for Nuclear Waste Regulatory Analyses
Southwest Research Institute

Self-affine properties of the ten standard profiles for the joint roughness coefficient (JRC), as proposed by Barton [1] for rock engineering practice and adopted by the International Society for Rock Mechanics (ISRM) [2], were analyzed using the theory of fractal geometry with the ultimate goal of relating the JRC values and the fractal properties of rock profiles. The semi-variogram method was adopted in the study for calculation of fractal properties. The validity of this method was tested using the fractional Brownian motion functions with Hurst exponent (H) varying from 0.5 to 0.9. A decreasing trend of JRC values with increase in fractal dimension was found for the Barton's ten profiles. This finding seems to suggest that fractal dimension may not be a good indicator of roughness of a rock joint. A good correlation was found between the intercept of the fractal model and the JRC values for the ten profiles and an empirical relation is suggested. This empirical relation appears to offer a viable method for estimating the JRC values for natural rock joints. Studies on the Apache Leap tuff joint profiles indicate that reasonably good estimation of the JRC values can be made using the suggested relation.

INTRODUCTION

A suitable measure of rock joint roughness is necessary to adequately describe rock joint behavior under both pseudostatic and dynamic shear conditions. The most commonly used measure of joint roughness in rock engineering practice is the joint roughness coefficient (JRC) proposed by N.R. Barton [1] and adopted by the International Society for Rock Mechanics (ISRM) [2]. This JRC concept has been implemented in a rock joint model developed by Barton and Choubey [3]. This rock joint model is able to adequately describe the unidirectional shear and dilation behavior of fresh rock joints [4], provided representative JRC values are used.

Barton and Choubey [3] proposed an approximation of the JRC by visually matching joint surface profiles with their ten "standard" ISRM profiles that range from 0 to 20. This approach is highly subjective [5,6]. To minimize this subjectivity, several methods have been proposed to link the JRC value with various aspects of the statistical characteristics of a rock joint to provide an objective alternative for JRC determination.

One of the approaches used for analyzing rock joint profiles is the theory of fractal geometry. Several researchers have proposed equations that correlate JRC values (which range from 0 to 20) of the ten ISRM profiles to their fractal dimensions. In the process of determining the fractal dimensions, the ten ISRM profiles were assumed to be self-similar [6,7,8]. This assumption implies that each profile is composed of several copies of itself with possible rotation and translation, scaled down from the original by a constant ratio r in all spatial directions. However, in reality, studies have shown that rock profiles or surface topographies are often self-affine fractals [9,10,11,12] that require different scaling factors in different directions.

In this paper, the self-affine properties of the ten ISRM profiles and the profiles of the natural rock joints from the Apache Leap site of Arizona are analyzed and discussed using the theory of fractal geometry. An empirical relationship between the intercepts of the fractal models and the related JRC values of the ten ISRM profiles is proposed. The usefulness of the empirical equation in estimating the JRC values of Apache Leap rock joints is also evaluated.

As discussed previously, rock profiles or surface topographies are often self-affine fractals and will require different scaling factors in different directions. Formally, points $X = (x,y)$ transform into new points $X' = (r_x x, r_y y)$ with $r_x = r_y H$ where H is the Hurst exponent and ranges between 0 and 1. There are several methods available for calculating the properties of a self-affine fractal. The semi-variogram method was used in this study.

The semi-variogram approach is used to characterize the spatial variability of random functions and is extremely well suited for describing random functions that are second-order stationary or appear to vary without bound [13]. The semi-variogram function is defined as the average of the sum of the squares of the differences of profile heights at a constant lag, h. It assumes zero means. The one-dimensional variogram function, $\gamma(h)$, can be expressed in a discrete form:

$$\gamma(h) = \frac{1}{2N} \sum_{i=1}^{N} \left[Z(x_i) - Z(x_i + h)\right]^2 \tag{1}$$

where $Z(x_i)$ is the height of the profile at location x_i, $Z(x_i+h)$ is the height of the profile at location x_i+h, h is the lag between two adjacent points, and N is the number of observations. The semi-variogram function, $\gamma(h)$, and the lag, h, shows a log-linear relationship:

$$\gamma(h) = I\, h^{\beta} \tag{2}$$

where I and β are constants, I can be defined also as an intercept at $h=1$. The fractal dimension, D, of a profile can be determined using the equation, $D = 2 - \beta/2$.

A FORTRAN computer program based on the semi-variogram method was written for fractal dimension calculation. The fractional Brownian motion functions with known fractal dimensions were used to verify this program. Generation of the fractional Brownian motion functions used the algorithm proposed by Saupe [14]. In this algorithm, the middle point between two known adjacent points is determined. This newly generated middle point then serves as a known point and the algorithm is repeated recursively until a desired number of points is obtained. A displacement, D_n, with desired variance is added to all the points at each step. D_n is given as [14]:

$$D_n^2 = \frac{1}{2}\sigma^2 \left(1 - \frac{1}{2^{2-H}}\right) \frac{1}{2^{2Hn}} \tag{3}$$

where n is the level of subdivision, H is the Hurst Exponent, and σ is the input standard deviation.

Five Hurst exponent H values ranging from 0.5 to 0.9 were chosen to generate the fractional Brownian motion functions that have fractal dimensions D from 1.1 to 1.5, where $D = 2 - H$. Figure 1 shows the five fractional Brownian motion functions with $\sigma = 1.0$. Figure 2 compares the H values calculated from the FORTRAN program with the actual H values used to generate the Brownian motion functions. It can be concluded from the figure that the semi-variogram method can be used to predict reasonably well the H value of each Brownian motion function, although there is a slight overestimation for rougher Brownian motion functions (corresponding to smaller H values) and underestimation for smoother Brownian motion functions (corresponding to larger H values) recognizing the fact that self-affinity is intrinsically difficult to measure on a finite sample.

EVALUATION OF BARTON'S TEN PROFILES

As discussed earlier, the JRC value is the most commonly used measure for representing joint roughness in various rock mechanics applications. The proposed ten profiles [1,2] represent JRC values from 0 to 20. Each profile covers a range of two scales of JRC; for example, from 0 to 2. In this study, a unique value was assigned to each profile for practicality; for example, 1 is assigned to a profile covering the JRC range of 0 to 2.

The ten profiles contained in '' `ISRM publication [2] were magnified `` about three times the size of the original plot, using a photocopier, for ease of digitization. The enlarged profiles were then digitized individually to create ten data sets. The upper boundary of each curve was used as the basis for digitizing. Only local peaks and valleys were digitized to give coordinates with respect to a selected horizontal datum. Consequently, the data interval in each of the data sets was not constant. For most of the profile curves, more than 300 points (locations) were digitized. The same unit length was used for both the horizontal and vertical axes. A small FORTRAN program was developed to rescale the data using the interpolating technique such that each data set has an equal data spacing and contains 512 data points. Equal spacing is necessary for using the semi-variogram method. Figure 3 shows the plot of the ten ISRM profiles regenerated using the final data sets. Comparison of the ten profile curves with the corresponding ones in the original ISRM publication [2] shows a remarkable similarity and can be considered representative.

Figure 4 shows the relation of the JRC values of the ten ISRM profiles and the corresponding fractal dimensions (solid circles) from the semi-variogram method in a log-log plot. Against common belief that a larger fractal dimension should correspond to a higher JRC value, a decreasing trend of the JRC values with increase in fractal dimension is shown in Figure 4. A similar result has also been reported by Sakellariou et al. [12] and Kulatilake et al. [15]. The variogram method was used by Kulatilake et al. [15] and the spectral method was used by Sakellariou et al. [12] to calculate the fractal dimensions of the ten ISRM profiles. Although the fractal dimensions reported by Sakellariou et al. [12] do not show a distinct decreasing trend, they did report unusually high fractal dimensions for the first five profiles. Sakellariou et al. [12] considered these relatively high values as erratic behavior and suggested that this behavior may be explained by the "quality of source material (smooth figures of a book) that causes mixing of noise in the signal in the raw data, a fact that cannot be overcome." While their postulation may be correct in general, it cannot explain the distinct and consistent trend of decreasing fractal dimension with increasing JRC value observed in Figure 4. The open circles in Figure 4 denote data from Apache Leap tuff joints. Related discussion will be provided later.

The finding that a higher JRC value corresponds to a smaller fractal dimension suggests that the use of fractal dimension alone for the characterization of the ten ISRM profiles is not sufficient since, according to the conventional wisdom, a rougher surface should yield a larger fractal dimension. Also, the fractal dimension only describes how the roughness varies with the scale of observation. It is the intercept, for example, the constant I in equation (2), or the crossover length that determines the steepness of the topography [16]. Figure 5 shows a distinct log-linear relation (solid circles) between the JRC values and the corresponding intercepts of the fractal models of the ten ISRM profiles. As can be observed from the figure, the intercept increases with the JRC values. Apache Leap tuff joints related data in Figure 5 (open circles) will be discussed later.

A multiple linear regression analysis was performed to determine the correlation among the JRC value, intercept, I, and fractal dimension, D. In this analysis, the logarithm of JRC was treated as a dependent variable whereas the logarithms of I and D were treated as independent variables. A regression equation to relate these three variables can be expressed as

$$JRC = 170 \, \frac{I^{0.654}}{D^{1.62}} \tag{4}$$

This equation has an adjusted R^2 value of 0.982 and a standard error of estimate of 0.0541. However, the analysis has indicated the presence of a sample-based multicollinearity between independent variables I and D. Action—such as collecting more data to break up the correlation or dropping one or more independent variables from the regression equation—will need to be taken to eliminate this multicollinearity. Since getting more data from the ten ISRM profiles is not possible, the only alternative is to drop one independent variable from equation (4). Testing the null hypothesis of the independent variables in the regression model of equation (4) indicates that the probability, P, of being wrong in concluding that there is a true association between the JRC and I is small with $P < 0.0001$. On the other hand, the probability of committing a Type I error is quite high, about 31%, in concluding that the JRC and D have a true correlation. A separate log-linear regression analysis of the JRC and D has concluded that the homoscedasticity (i.e., constant variance) assumption has been violated. Homoscedasticity is one of the three basic assumptions made in conducting a linear regression analysis. This violation suggests that a different model should be considered. The results

of the multiple and the separa*- log-linear regressions pointed to a 'ogical conclusion that the fractal
dimension, D, is redundant and should be dropped from the regression model of equation (4).

The log-linear regression model for the JRC and I can be expressed as

$$JRC = 195 \, I^{0.737} \tag{5}$$

The adjusted R^2 value for this correlation is 0.981 and the standard error of estimate 0.0548. Note that the
adjusted R^2 values for equations (4) and (5) are essentially the same and the difference between the two
standard error of estimates is small, further suggesting that the intercept, I, alone is sufficient for predicting
JRC. This regression model is represented in Figure 5 as a solid line. The two broken lines on the sides of
the regression line give the prediction interval at a 95% confidence level of the regression line. This
prediction interval, also called the confidence interval for the population, describes the range where the data
values will fall 95% of the time for repeated measurements.

It is well-known that two parameters, namely I and D, will be needed to uniquely characterize the fractal
model of a rough profile in log-log space [9,16,17,18]; due to the complexity of natural rock joint surfaces,
it is possible that D may not be a constant value or may be a constant only over a limited range of scales
[19]. As discussed earlier, D represents the variation of surface elevation at different scales and the variance
or the deviation from the mean elevation associated with a profile is represented by I [17]. In other words,
I is more representative of the primary asperities with long wavelengths that are believed to control the actual
shear behavior of natural rock joints, while D seems to represent the higher order asperities that have a
secondary effect on rock joint shear behavior [18]. In the past, most of the focus on characterizing rock joint
surfaces for engineering practices has been on relating the fractal dimension with the associated JRC values
[6,7, 8,12,19]. This approach may have ignored one fundamental and important aspect of rock joint
roughness. Only recently, the importance of I or primary asperities of a rock joint has been emphasized and
considered in the development of joint shear models [15,17,20]. The analysis performed here on the ten
ISRM profiles further suggests that the intercept, I, alone may offer a reasonable approximation for various
applications in the rock mechanics field, using the expression proposed in equation (5), in determining the
JRC values of rock joints. In the following discussion, the usefulness of equation (5) for the determination
of the JRC values of Apache Leap rock joints is evaluated.

APPLICABILITY EVALUATION OF EQUATION (5)

Rock profile measurements and experimental procedures

The rock joint specimens used in this study were collected from the Apache Leap site near Superior,
Arizona. The rock at this site is a vitrified and densely welded tuff. Each specimen consists of two mated
rock blocks with a natural joint interface between them. The top block of the specimen is about 203 mm in
length and width and about 102 mm in height. The bottom block is about 305 mm long, 203 mm wide, and
102 mm high.

Before the two blocks of a jointed specimen were grouted into the steel shear boxes that are part of fixtures
of a dynamic shear test apparatus, measurements of rebound numbers using a Schmidt hammer were taken
on both joint surfaces and on the sides of both blocks. A discussion regarding the direct shear test apparatus,
which can simulate controlled dynamic motions, is provided elsewhere [21]. Immediately following the
Schmidt hammer tests, tilt tests were performed to determine the tilt angle of the joint along both the
projected direction of shear and its reverse direction. The two blocks were then grouted into their respective
specimen steel boxes that house the joint specimen during the direct shear test, and subsequently put into an
oven at 102°C for 24 hr to accelerate the curing of the grout. The thickness of the grout between the shear
box and the rock block is about 12.7 mm.

After heating both joint surfaces, profile measurements were taken. The profile measurement was taken
using a non-contact surface height gauging profilometer. This profilometer consists of an Asymtek benchtop
gantry type X-Y-Z positioner and a Keyence laser displacement meter attached to the Z-axis of the positioner.
This laser displacement meter includes a red visible laser head that has a displacement measurement
resolution of about 0.5 micrometer. The profilometer movements were controlled by personal computer (PC)

commands to the A-102B X-Y ⁊ table via a serial port. The A-102ᴿ ʼable had a built-in computer for interpreting high-level commands from the PC and then executing the moves. A custom computer program written in Borland's Turbo C was used to issue movement commands to the A-102B, to read the displacement measurement Z-axis movement from the LC-2100, and to format and store pertinent scanning and rock joint profile displacement information to a hard-drive data file. For both blocks, profiles were measured along more than 140 longitudinal sections at an interval of 1.27 mm between the two consecutive sections. For each longitudinal profile section, measurements were taken at an interval of 1.27 mm.

Twenty-two direct shear tests on single-joint rock specimens have been performed. Sixteen of them were carried out under pseudostatic loading conditions, two were carried out under harmonic loading conditions, and four were tested under simulated earthquake loading conditions. Before the shear test started, a joint was subjected to five normal loading and unloading cycles to bring the mated blocks to their assumed undisturbed state. The shear tests, under various constant normal loads, were displacement controlled and the results of these tests are reported elsewhere [22].

Calculation of JRC using laboratory shear test results

JRC values of the twenty-two single-joint rock specimens were calculated from the corresponding shear test results using the following equation [3]:

$$\tau = \sigma_n \tan \left[JRC \log \left(\frac{JCS}{\sigma_n} \right) + \phi_r \right] \tag{6}$$

where τ is the joint shear strength, σ_n is the applied normal stress, JCS is the joint wall compressive strength, and ϕ_r is the joint residual angle of friction. JCS and ϕ_r need to be calculated separately by using the following two equations [3] which may introduce some uncertainties into the determination of JRC.

$$\log (JCS) = 0.00088 \gamma r_e + 1.01 \tag{7}$$

$$\phi_r = (\phi_b - 20^\circ) + 20 \left(\frac{r_e}{R_e} \right) \tag{8}$$

where γ is the rock density, ϕ_b is the basic friction angle, and r_e and R_e are the rebound numbers from Schmidt hammer tests on joint wall and smooth rock surface, respectively. From a tilt test of one rock cylinder sliding down the other [23] ϕ_b was estimated. The JRC values for the twenty-two rock joints, back-calculated from the results of direct shear tests using equation (6), are given in Table 1.

Self-affine fractal properties of rock joint profiles

The same FORTRAN computer program used for evaluating the ten ISRM profiles was used to determine the self-affine properties of the Apache Leap tuff joints. Each profile along the direction of shear for both the top and bottom blocks of a joint specimen was analyzed to determine the fractal dimension and intercept. The representative fractal dimension and intercept of the joint specimen, which are assumed to be the arithmetic average of all profiles, are given in Table 1.

Examination of fractal properties

The relation between the JRC values and the corresponding fractal dimensions of the twenty-two Apache Leap tuff joints is shown in Figure 4 (hollow circles). It is interesting to note that, consistent with the observation made for the ISRM profiles, the fractal dimensions of the Apache Leap joints, in general, exhibit a decreasing trend with an increase in JRC values, although they show wider scattering than those of the ISRM profiles. This result is consistent with the findings reported by Miller et al. [11] on rock joint surfaces of basalt, gneiss, and quartizite. Figure 4 also shows that the fractal dimensions calculated from the Apache

Leap joint profiles are consistent and substantially larger than those of ISRM profiles with the same JRC values. This observation suggests that the relation between the fractal dimensions and JRC values of the ten ISRM profiles will not be appropriate for predicting the JRC values of Apache Leap joints because such predictions will lead to unrealistically low JRC. The plot for the intercepts of fractal models of the Apache Leap joints and the associated JRC values is shown in Figure 5 as open circles. As can be seen, the majority of the data points fall within or near the range of the 95% prediction interval of the regression model of equation (5), an indication that a reasonably good estimation of the JRC values can be made using equation (5) for the Apache Leap tuff joints. It should be noted that the form of semi-variogram used in this study is often highly sensitive to sampling direction and sampling interval [24]. Therefore, the same sampling procedure that has been discussed earlier in this paper for obtaining profile data of the Apache Leap tuff joints should be followed if equation (5) is to be used properly.

CONCLUSIONS

The ten ISRM profiles associated with the JRC concept and several Apache Leap tuff joints were analyzed using the theory of fractal geometry and the semi-variogram method. The result shows a consistent trend that a profile with a higher JRC value seems to have a smaller fractal dimension. For practical engineering applications, the intercept of the fractal model of a profile or rock joint is found to be adequate for representing the roughness of the profile. A good correlation has been found between the JRC values and associated intercepts, I, of fractal models of the ten ISRM profiles. An empirical equation relating the JRC and I is proposed. This equation appears to give a reasonably good estimation of the JRC values of the Apache Leap tuff joints and may offer a reasonable alternative for the prediction of those of other natural rock joints. Further investigation is recommended for extending the proposed equation, and verifying its applicability, to rock joints of other rock types.

REFERENCES

1. Barton N.R. Review of a new shear strength criterion for rock joints. *Engineering Geology,* 7, 287–332 (1973).
2. International Society for Rock Mechanics (ISRM). Suggested methods for the quantitative description of discontinuities in rock masses. *Int. J. Rock Mech. Min. Sci. & Geomech. Abstr.,* 15, 319–368 (1978).
3. Barton N.R. and Choubey V. The shear strength of rock joints in theory and practice. *Rock Mechanics,* 10, 1–54 (1977).
4. Hsiung S.M., Ghosh A., Chowdhury A.H., and Ahola M.P. *Evaluation of rock joint models and computer code UDEC against experimental results.* NUREG/CR-6216, U.S. Nuclear Regulatory Commission, Washington, DC (1994).
5. Miller S.M., McWilliam P.C., and Kerkering J.C. Evaluation of stereo digitizing rock fracture roughness. *Rock Mechanics as a Guide for Efficient Utilization of Natural Resources,* A.W. Khair, ed., Balkema, Rotterdam: Netherlands, 201–208 (1989).
6. Wakabayashi N. and Fukushige I. Experimental study on the relation between fractal dimension and shear strength. *Conf. Fractured and Jointed Rock Masses,* Preprints, Lake Tahoe, CA (1992).
7. Turk N., Greig M.J., Dearman W.R., and Amin F.F. Characterization of rock joint surfaces by fractal dimension. *28th U.S. Symp. on Rock Mechanics,* Tucson, AZ: University of Arizona, 1,223–1,236 (1987).
8. Lee Y.-H., Carr J.R., Barr D.J., and Haas C.J. The fractal dimension as a measure of the roughness of rock discontinuity profiles. *Int. J. Rock Mech. Min. Sci. & Geomech. Abstr.,* 27, 453–464 (1990).

9. Brown S.R. and Scholz C⁻⁻ Broad bandwidth study of the topr ⁿphy of natural rock surfaces. *J. Geophys. Res.*, **90(B14)**, 12,575–12,582 (1985).

10. Malinverno A. A simple method to estimate the fractal dimension of a self-affine series. *Geophys. Res. Let.* **17(11)**, 1,953–1,956 (1990).

11. Miller S.M., McWilliam P.C., and Kerkering J.C. Ambiguities in estimating fractal dimensions of rock fracture surfaces. *Rock Mechanics Contributions and Challenges*, W.A. Hustrulid and G.A. Johnson eds., Balkema, Rotterdam: Netherlands, 471–478 (1990).

12. Sakellariou M., Nakos B., and Mitsakaki C. On the fractal character of rough surfaces. *Int. J. Rock Mech. Min. Sci. & Geomech. Abstr.*, **28(6)**, 527–533 (1991).

13. Oliver M.A. and Webster R. Semi-variograms for modelling the spatial pattern of landform and soil properties. *Earth Surface Processes and Landforms*, **11**, 491–504 (1986).

14. Saupe D. Algorithms for random fractals. *The science of fractal images*. H. Peitgen and D. Saupe, eds., Springer-Verlag, New York, 71–136 (1988).

15. Kulatilake P.H.S.W., Shou G., and Huang T.H. A variogram/fractal based new peak shear strength criterion for rock joints. *35th U.S. Sym. on Rock Mechanics*, Reno, NV: University of Nevada, Reno, 653–658 (1995).

16. Power W.L. and Tullis T.E. Euclidean and fractal models for the description of rock surface roughness. *J. Geophys. Res.*, **96(B1)**, 415–424 (1991).

17. Ghosh A. and Hsiung S.M. On characterization of self-affine fractal profiles. *Proc. 10th Conf. of Eng. Mech.*, Boulder, Colorado, 179–182 (1995).

18. Hsiung S.M., Ghosh A., and Chowdhury A.H. On natural rock joint profile characterization using self-affine fractal approach. *35th U.S. Sym. on Rock Mechanics*, Reno, NV: University of Nevada, Reno, 681–687 (1995).

19. Carr J.R. and Warriner J.B. Relationship between the fractal dimension and joint roughness coefficient. *Bull. Association of Engineering Geologists*, **XXVI(2)**, 253–263 (1989).

20. Seidel J.P. and Haberfield C.M. The use of fractal geometry in a joint shear model. *Mechanics of Jointed and Faulted Rock*, H.P. Rossmanith ed., Balkema, Rotterdam: Netherlands, 529–534 (1995).

21. Kana D.D., Chowdhury A.H., Hsiung S.M., Ahola M.P., Brady B.H.G., and Philip J. Experimental techniques for dynamic shear testing of natural rock joints. *Proc. 7th Int. Congress on Rock Mech.*, Aachen, Germany, 519–526 (1991).

22. Hsiung S.M., Kana D.D., Ahola M.P., Chowdhury A.H., and Ghosh A. *Laboratory characterization of rock joints*. NUREG/CR-6178, U.S. Nuclear Regulatory Commission, Washington, DC (1994).

23. Barton N.R., Bandis S., and Bakhtar K. Strength, deformation and conductivity coupling of rock joints. *Int. J. Rock Mech. Min. Sci. & Geomech. Abstr.*, **22**, 121–140 (1985).

24. Burrough P.A. Fractal dimensions of landscapes and other environmental data. *Nature*, **294**, 240-242 (1981).

Table 1 Estimated JRC, intercept (I), and fractal dimension (D) for Apache Leap tuff joints

| Test No.	JRC	I, mm^2	D	Test No.	JRC	I, mm^2	D
1	12.0	0.0293	1.245	12	11.9	0.0200	1.395
2	13.4	0.0291	1.352	13	11.2	0.0170	1.329
3	10.8	0.0221	1.296	14	11.1	0.0211	1.279
4	9.8	0.0163	1.276	15	19.8	0.0184	1.302
5	11.6	0.0143	1.365	16	18.8	0.0309	1.415
6	10.5	0.0144	1.310	17	19.4	0.0314	1.214
7	12.1	0.0164	1.274	18	12.5	0.0152	1.257
8	11.0	0.0152	1.290	19	11.2	0.0161	1.297
9	7.1	0.0080	1.317	20	16.7	0.0397	1.301
10	11.8	0.0197	1.260	21	14.4	0.0247	1.183
11	10.4	0.0082	1.302	22	19.3	0.0355	1.272
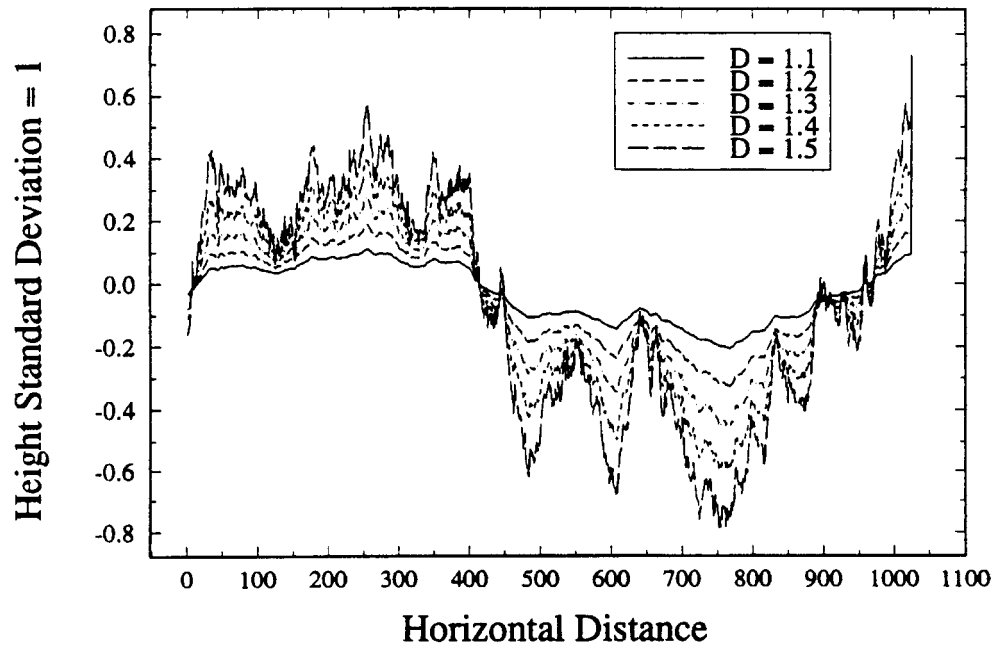
Figure 1   Generated self-affine profiles
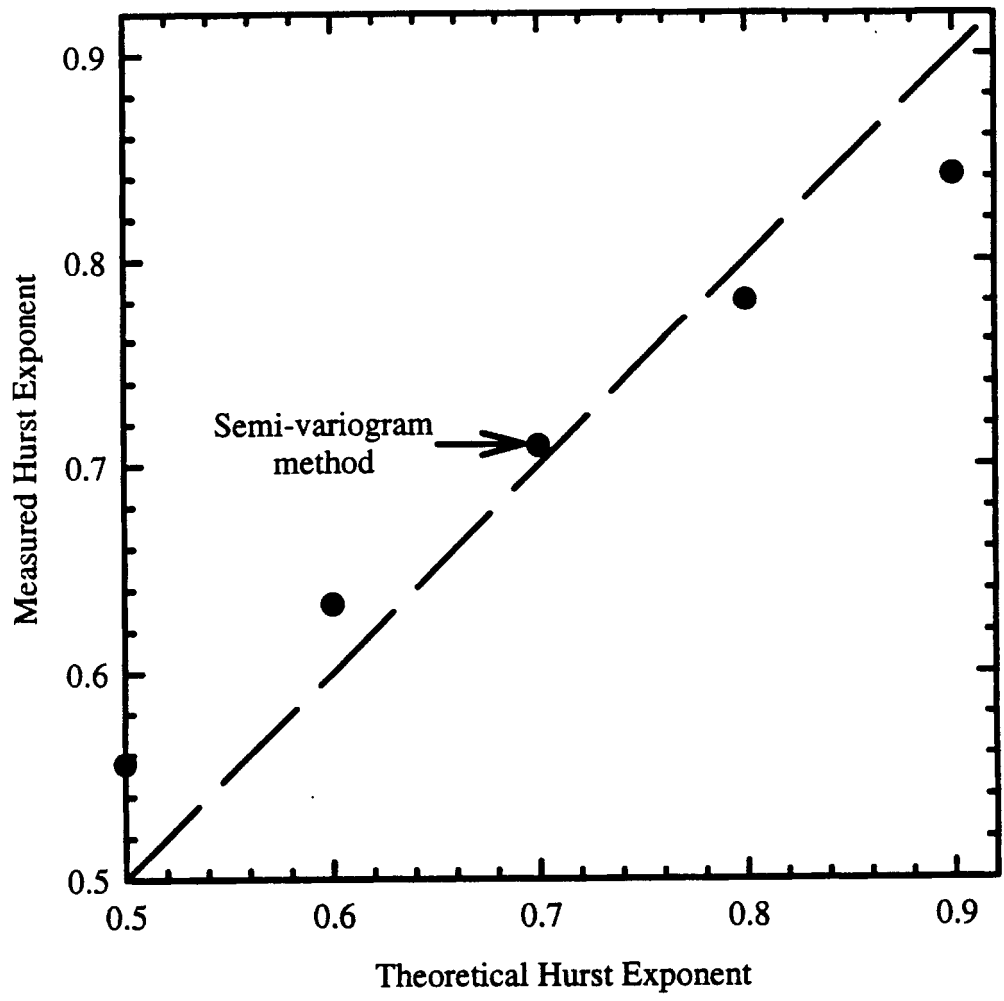
Figure 2   Comparison of Hurst exponents calculated using semi-variogram method with the expected values

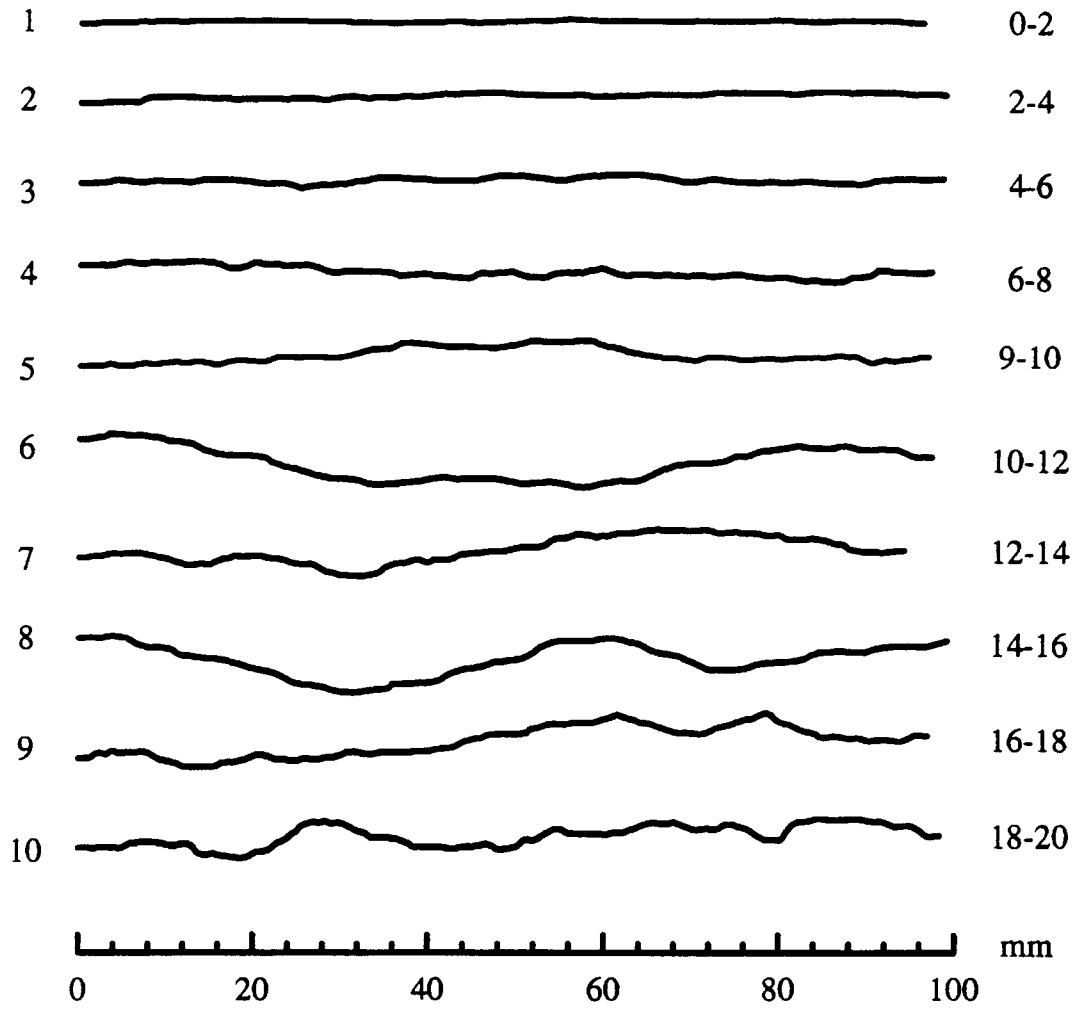# TYPICAL ROUGHNESS PROFILES for JRC range:

1	_____	0-2
2	_____	2-4
3	_____	4-6
4	_____	6-8
5	_____	9-10
6	_____	10-12
7	_____	12-14
8	_____	14-16
9	_____	16-18
10	_____	18-20

0   20   40   60   80   100   mm

Figure 3   ISRM roughness profiles and associated JRC ranges
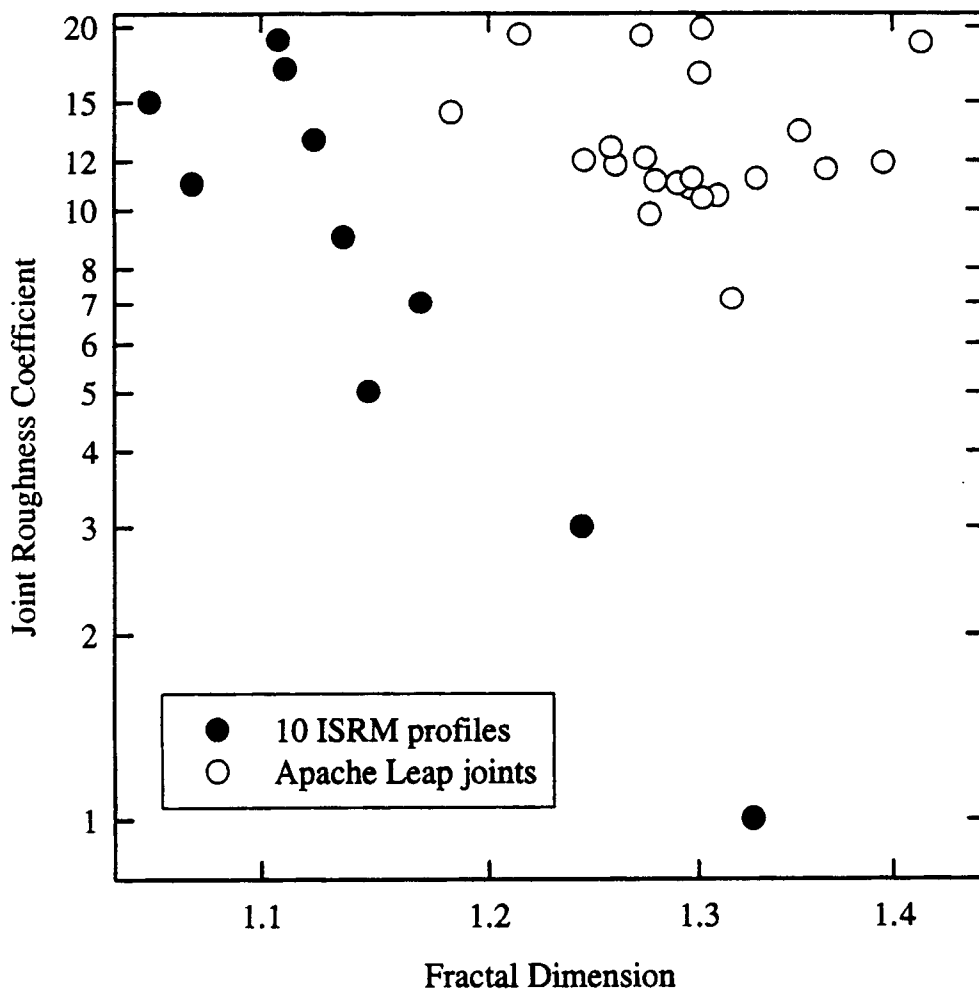
Figure 4   Relation of joint roughness coefficient and corresponding fractal dimension for 10 ISRM and Apache Leap joint profiles
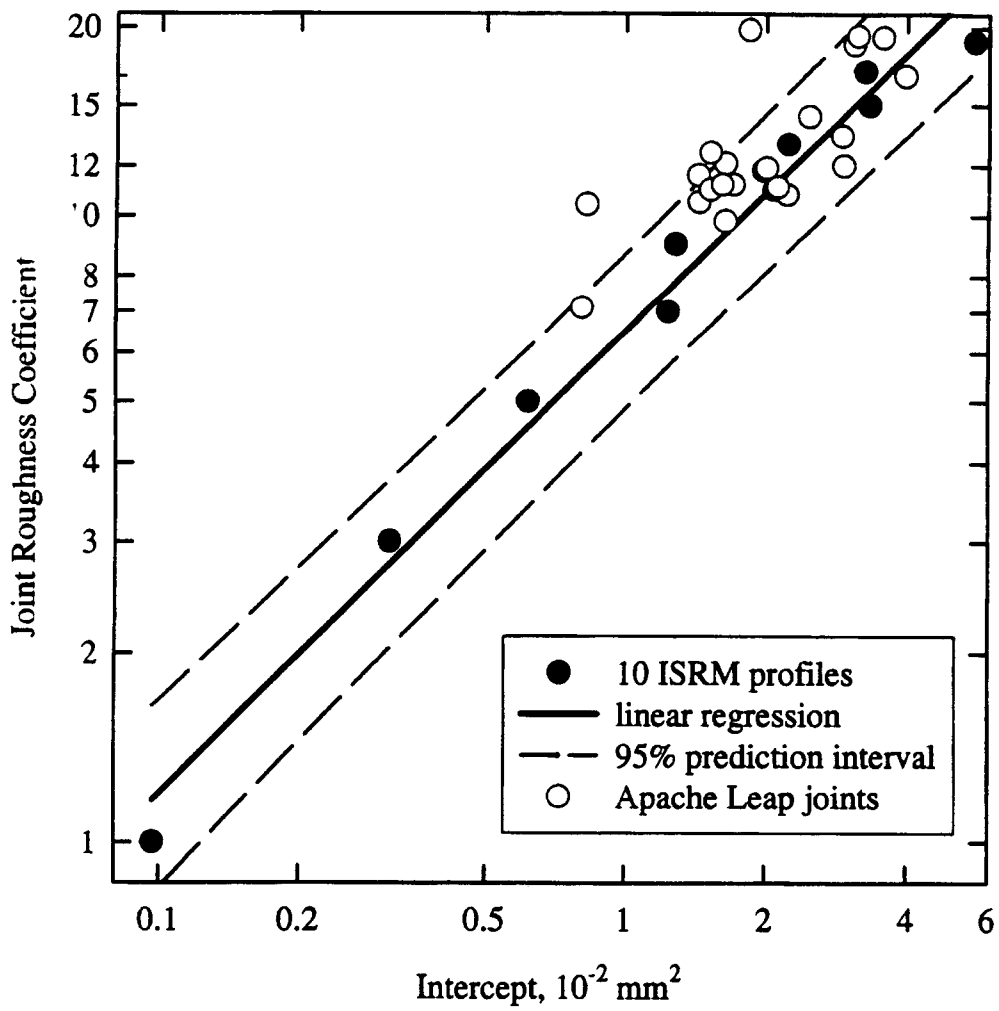
Figure 5   Relation of joint roughness coefficient and corresponding fractal intercept for 10 ISRM and Apache Leap joint profiles